Hindawi Publishing Corporation
International Journal of Oceanography
Volume 2012, Article ID 531982, 9 pages
doi:10.1155/2012/531982

Research Article

Observation of Oceanic Eddy in the Northeastern Arabian Sea Using Multisensor Remote Sensing Data

R. K. Sarangi

Marine Geo and Planetary Sciences Group, Space Applications Centre (ISRO), Ahmedabad 380 015, India

Correspondence should be addressed to R. K. Sarangi, sarangi74@yahoo.com

Received 3 November 2011; Revised 21 February 2012; Accepted 26 April 2012

Academic Editor: Renzo Perissinotto

An oceanic eddy of size about 150 kilometer diameter observed in the northeastern Arabian Sea using remote sensing satellite sensors; IRS-P4 OCM, NOAA-AVHRR and NASA Quickscat Scatterometer data. The eddy was detected in the 2nd week of February in Indian Remote Sensing satellite (IRS-P4) Ocean Color Monitor (OCM) sensor retrieved chlorophyll image on 10th February 2002, between latitude 16°90′–18°50′N and longitude 66°05′–67°60′E. The chlorophyll concentration was higher in the central part of eddy (~1.5 mg/m^3) than the peripheral water (~0.8 mg/m^3). The eddy lasted till 10th March 2002. NOAA-AVHRR sea surface temperature (SST) images generated during 15th February-15th March 2002. The SST in the eddy's center (~23°C) was lesser than the surrounding water (~24.5°C). The eddy was of cold core type with the warmer water in periphery. Quickscat Scatterometer retrieved wind speed was 8–10 m/sec. The eddy movement observed southeast to southwest direction and might helped in churning. The eddy seemed evident due to convective processes in water column. The processes like detrainment and entrainment play role in bringing up the cooler water and the bottom nutrient to surface and hence the algal blooming. This type of cold core/anti-cyclonic eddy is likely to occur during late winter/spring as a result of the prevailing climatic conditions.

1. Introduction

Eddies are small features with a big impact. They are where a lot of ocean physics happen and are an integral part of our climate system. Coastal eddies have a major role in regulating the weather near the shore and they are important for fisheries. In the open ocean, eddies bring nutrient-rich cold water up to the surface and are an important part of the global carbon cycle [1]. These eddies are rotating masses of water that have broken off from a strong front. Eddies are crucial to the transport of heat, momentum, trace chemicals, biological communities, the oxygen, and nutrients relating to life in the sea [2]. They are also active in air-sea interaction, both through response to weather and in shaping the patterns of warmth that drives the entire atmospheric circulation. Measurements of ocean color and the fate of light in the ocean are extremely useful for describing biological dynamics in surface waters [3–5]; thus the oceanographic communities has made a substantial commitment to remote sensing of ocean color from space [6, 7]. Regional scale ocean color imageries are particularly useful for space-borne studies of ocean margins because of the importance and dominance of mesoscale features (upwelling plumes, eddies, filaments, and river plumes) in continental shelf and slope waters [8]. The oceanic and coastal processes rapidly alter the optical properties of waters and these effects get manifested in the color of the water [9].

Recent study over South China Sea describes the three-dimensional dynamic structure of eddy on the basis of the analyses of *in situ* current, hydrographic measurements, and concurrent satellite observations. That is important in the development, sustenance, and dissipation of cold eddies in the ocean [10]. Oceanic circulation, stratification, and eddies have been studied using scatterometer data [11]. A cyclonic eddy was observed around the mooring location of the Marine Optical Buoy (MOBY) offshore of Lanai Island, Hawaii. The satellite observations such as the sea surface temperature (SST) and the chlorophyll concentration were analyzed and the cold core cyclonic eddy displayed a significant increase in surface chlorophyll [12]. Eddies are thus usually associated with high biological activity, as reported in several papers during the past decade [13–20]. However, the eddies

role in the biological and biogeochemical processes remain enigmatic, partially because of the challenges of *in situ* eddy measurements due to the spontaneity in eddy generation and present technological limitations [21]. Chlorophyll-a (Chl-a) concentration, an index of phytoplankton biomass, is the most important property of the marine ecosystem. Remote sensing images of ocean color, converted into Chl-a concentration, provide a window into the ocean ecosystem with synoptic scales. It is a promising approach for understanding the oceanic biological and physical processes and for monitoring ocean waters [22–24].

The Arabian Sea is unique among low-latitude sea by terminating at latitude of 25°N and being under marked continental influence. It is the region of monsoon and its biological production is affected by the physical processes altering the vertical flux of nutrients in the mixed layer [25]. Satellite-based observations on ocean color provides a tool to monitor the biological productivity in terms of phytoplankton concentration. Remote sensing images of ocean color, converted into chl-a concentration, provide a window into the ocean ecosystem with synoptic scales [2]. The biological processes are being manifested by the physical events in the sea, like their circulation patterns and other surface features caused due to wind and ocean currents. These physical processes are relevant to ocean color studies. Remote sensing technique offers a practical tool in overcoming the problems like regular *in situ* observations of physical and biological processes linked to surface ocean and relevant data analysis [26, 27].

2. Objectives of the Study

(i) Analysis of the IRS-P4 OCM data for the northeastern Arabian Sea during the period February-March 2002 and detection of eddy using chlorophyll images and monitoring the phases of the eddy;

(ii) analysis of the NOAA-AVHRR data for the northeastern Arabian Sea during the period February-March 2002 to retrieve Sea Surface Temperature (SST) images and correlate the OCM derived chlorophyll images with SST images;

(iii) analyze the NASA Quickscat scatterometer retrieved wind speed and wind vector data for the above period over northeast Arabian Sea and interpret the direction and magnitude of the eddy.

3. IRS-P4 OCM Sensor

The ocean color monitor (OCM) of the Indian Remote Sensing satellite IRS-P4 is optimally designed for the estimation of chlorophyll in coastal and oceanic waters, detection and monitoring of phytoplankton blooms, studying the suspended sediment dynamics, and the characterization of the atmospheric aerosols. IRS-P4 satellite carrying onboard remote sensing payload Ocean Color Monitor (OCM) was launched successfully by Polar Satellite Launch Vehicle (PSLV) on May 26, 1999 from Sriharikota, India. The technical specifications of the OCM sensor are mentioned in Table 1 [28].

Table 1: Technical characteristics of IRS-P4 OCM payload.

Spectral range	404–882 nm
no. of channels	8
Wavelengths range (nm) and Signal to noise ratio (SNR)	Channel 1: 404–423 (340.5)
	Channel 2: 431–451 (440.7)
	Channel 3: 475–495 (427.6)
	Channel 4: 501–520 (408.8)
	Channel 5: 547–565 (412.2)
	Channel 6: 660–677 (345.6)
	Channel 7: 749–787 (393.7)
	Channel 8: 847–882 (253.6)
Satellite altitude (km)	720
Spatial resolution (m)	360 × 236
Swath (km)	1420
Repeativity	2 days
Quantisation	12 bits
Equatorial crossing time	12 noon
Along track steering (to avoid sunglint)	20°

4. OCM Data Processing

The retrieval of ocean color parameters, such as phytoplankton pigment (chlorophyll-a) in oceanic waters, involves two major steps, the first being atmospheric correction of visible channels to obtain normalized water leaving radiances in shorter wavelengths and second application of the bio-optical algorithm for retrieval of phytoplankton pigment concentration.

4.1. Atmospheric Correction of the IRS-P4 OCM Imagery. In the ocean remote sensing, the signal received at the satellite altitude is dominated by radiances contribution through atmospheric scattering processes and only 8–10% signal corresponds to oceanic reflectance. Therefore, it has been mandatory to correct the atmospheric effect to retrieve any quantitative parameter from space. The OCM scenes were corrected for atmospheric effects of Rayleigh and aerosol scattering using an approach called long wavelength atmospheric correction method. The approach used the two near infra red channels at 765 and 865 nm to correct for the contribution of molecular and aerosol scattering in visible wavelengths at 412, 443, 490, 510, and 555 nm [29–31]. The water leaving radiances derived from atmospheric correction procedure was used to compute chlorophyll-a pigment concentration.

4.2. Chlorophyll Algorithm. A number of bio-optical algorithms for retrieval of chlorophyll have been developed to

relate measurements of ocean radiance to the *in situ* concentrations of phytoplankton pigments. O'Reilly and Maritorena et al. [32] proposed an empirical algorithm (also known as Ocean Chlorophyll 2 or OC2) and operated successfully on SeaWiFS ocean color data. This algorithm captures the inherent sigmoid relationship. The algorithm operates with five coefficients and has following mathematical form:

$$C = -0.071 + 10^{(0.319 - 2.336 * X + 0.879 * X^2 - 0.135 * X^3)}, \quad (1)$$

where C is chlorophyll concentration in mg/m^3 and $X = \log_{10}[R_{rs}490/R_{rs}555]$. R_{rs} is remote sensing reflectance. This algorithm has been presently used for generating the chlorophyll maps, using IRS-P4 OCM-derived water leaving radiances. The chlorophyll retrieval accuracy obtained is within ±30% [33].

5. Dataset Used

Fourteen date chlorophyll images were generated using the above mentioned procedure from the cloud-free passes of IRS-P4 OCM sensor during the period February-March 2002 covering the offshore water in the northeast Arabian Sea. The consecutive cloud-free passes were selected during February 10, 2002 to March 10, 2002. The chlorophyll images were geometrically corrected and gridded with 3.0 degree latitude and longitude interval. The path 9 and row 13, 14 scenes of IRS-P4 OCM data were processed and chlorophyll images were generated for each day and two pass images were mosaiced. Similarly, NOAA-AVHRR data were processed during the above period to retrieve and visualize the SST images. The Quickscat data product received from PO.DAAC, JPL/NASA website were processed and plotted to retrieve the wind speed and wind vector products during February 15, 2002 to March 15, 2002.

6. Methodology for SST Retrieval

The SST retrieval using AVHRR Channels 4 and 5 was performed using following three steps.

6.1. Radiometric Calibration. It was done to convert the channel 4 and 5 digital data into brightness temperatures. It was assumed that the output of each channel (in counts) is a linear function to sensed radiances. The function is defined as

$$N = G * X + I, \quad (2)$$

where N is the radiance of target at count value X, G and I are gain and intercept, respectively. The brightness temperature (T_b) was obtained using Planck's radiation equation:

$$T_b = \frac{C_2 n}{\ln[1 + (C_1 n^3/N)]}, \quad (3)$$

where, $C_1 = 1.1910659 * 10^{-5}$ Cm·K and $C_2 = 1.1438833$ Cm·K.

6.2. SST Computation. Using McClain's algorithm [34–36]

$$\text{SST} = 3.6569 * T_{11} - 2.6705 * T_{12} - 268.92, \quad (4)$$

where, T_{11} and T_{12} are the brightness temperatures for the central wavelength 11 and 12 μm of the channels 4 and 5. The NOAA-AVHRR retrieved SST has been validated for Indian Ocean region and found to be within well accuracy range, ±0.5°C [37].

6.3. Geometric Correction. It is performed using the Ground Control Points (GCPs) resampled from the master image to the AVHRR image and Mercator projection is applied.

7. Results and Discussion

The eddy was detected in the 2nd week of February in IRS-P4 OCM derived chlorophyll image on 10th February 2002 covering latitudes 16°90′–18°50′N and longitudes 66°05′–67°60′E (Figure 1). During this period, several phytoplankton bloom features were seen in the northeast Arabian Sea. The chlorophyll concentration was found to be higher in the central part of the eddy (~1.5 mg/m^3) than the peripheral water around the eddy (~0.8 mg/m^3) as observed in the image. Analysis has been done with three locations along the eddy region (Eddy core, 19.58°N and 68.27°E; eddy periphery, 19.60°N and 67.94°E and outside eddy, 19.00°N and 69.21°E). There has been observation of increase in the chlorophyll concentration (1.10 mg/m^3) in the eddy core and in the periphery region as compared to the outer region of eddy (Figure 2). With the movement of the eddy, the outer region observed to be spread along with eddy region and chlorophyll concentration in late stage indicates the dissipation of eddy. The chlorophyll concentration decreases to 0.14 mg/m^3 (Figure 2). The eddy appeared as a circular concentric structure which lasted for a month period till 10th March 2002. The eddy was spread for about 150 km diameter. The eddy appeared to be cold core type as the central part was more productive may be due to lesser temperature than its peripheral water. The eddy was at its peak during 22nd February–6th March 2002 and then subsequently its size and diameter reduced. The surrounding water showed the disappearance of bloom patches.

To study the relationship of the eddy with sea surface temperature (SST), NOAA Advanced very high-resolution radiometer (AVHRR) sensor-retrieved SST images were studied during the period 15th February 2002–15th March 2002 (Figure 3). The SST images detected the eddy's appearance with lower temperature in the eddy's center (~23°C) than the water surrounding the eddy (~24.5°C). There was a significant SST gradient of 1.5°C observed in the SST images, around the eddy. The feature was consistent during a month period as compared to the IRS-P4 OCM-retrieved chlorophyll images. So, the eddy was confirmed to be cold core type with the warmer surrounding water in periphery. The movement of eddy appeared to be in clockwise direction and it was an anticyclonic eddy. These results were being interpreted with NASA Quickscat scatterometer retrieved wind vector data (Figure 4). The average wind speed was about 10 cm/sec

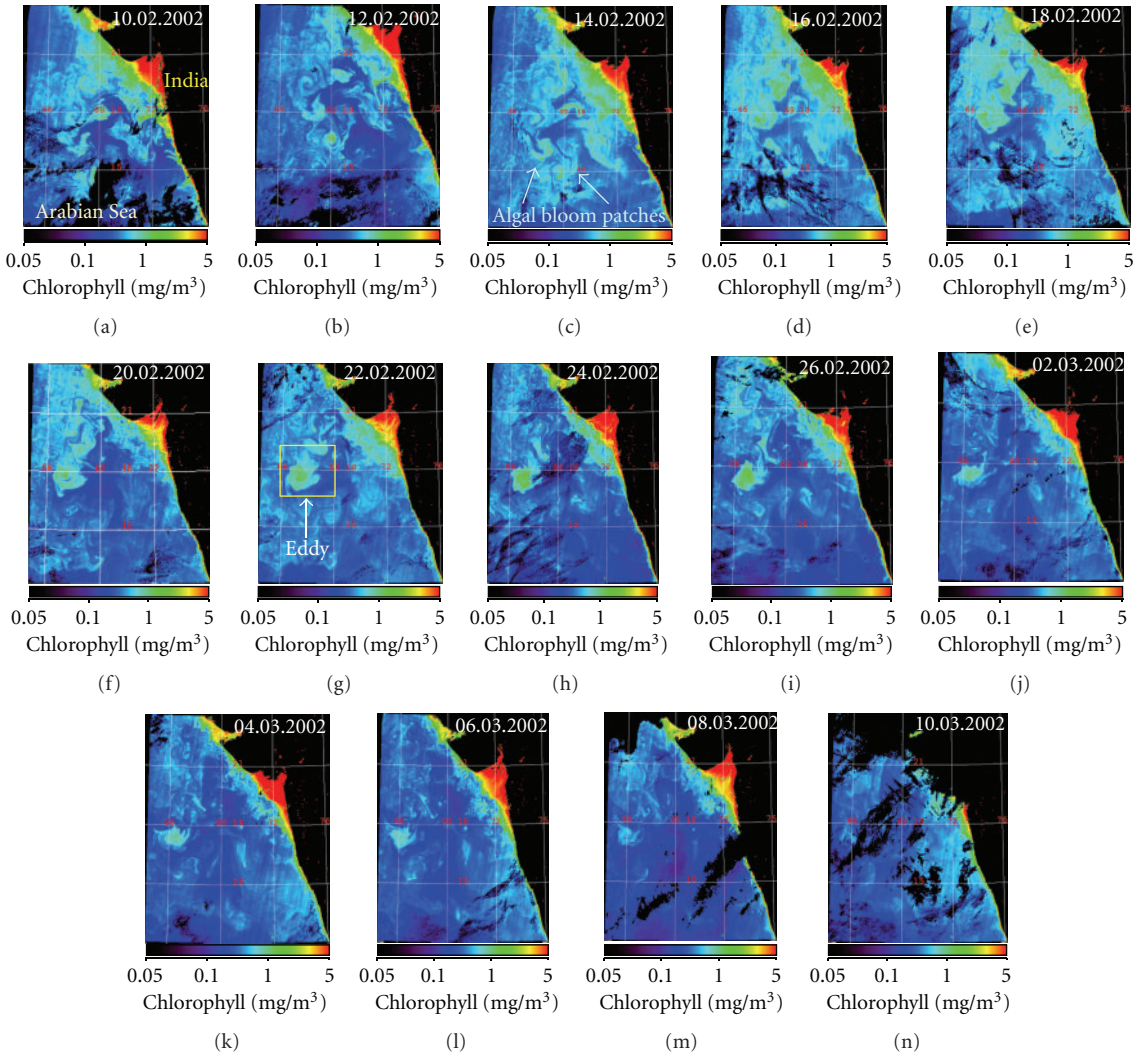

Figure 1: IRS-P4 OCM-derived chlorophyll images for February-March 2002 showing the eddy in different stages in the northeast Arabian Sea.

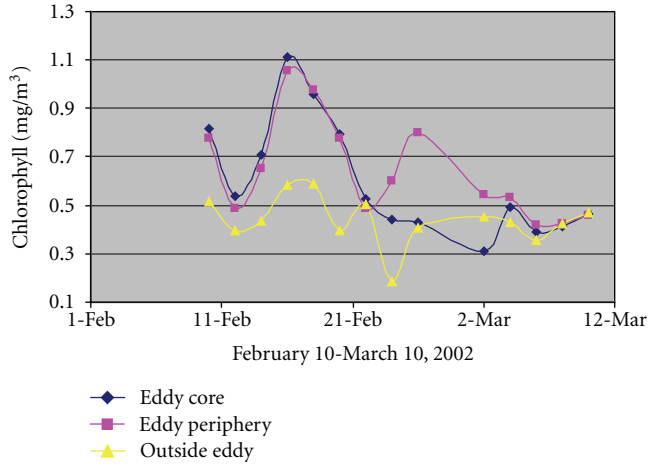

Figure 2: Observation of OCM derived chlorophyll concentration along the eddy region.

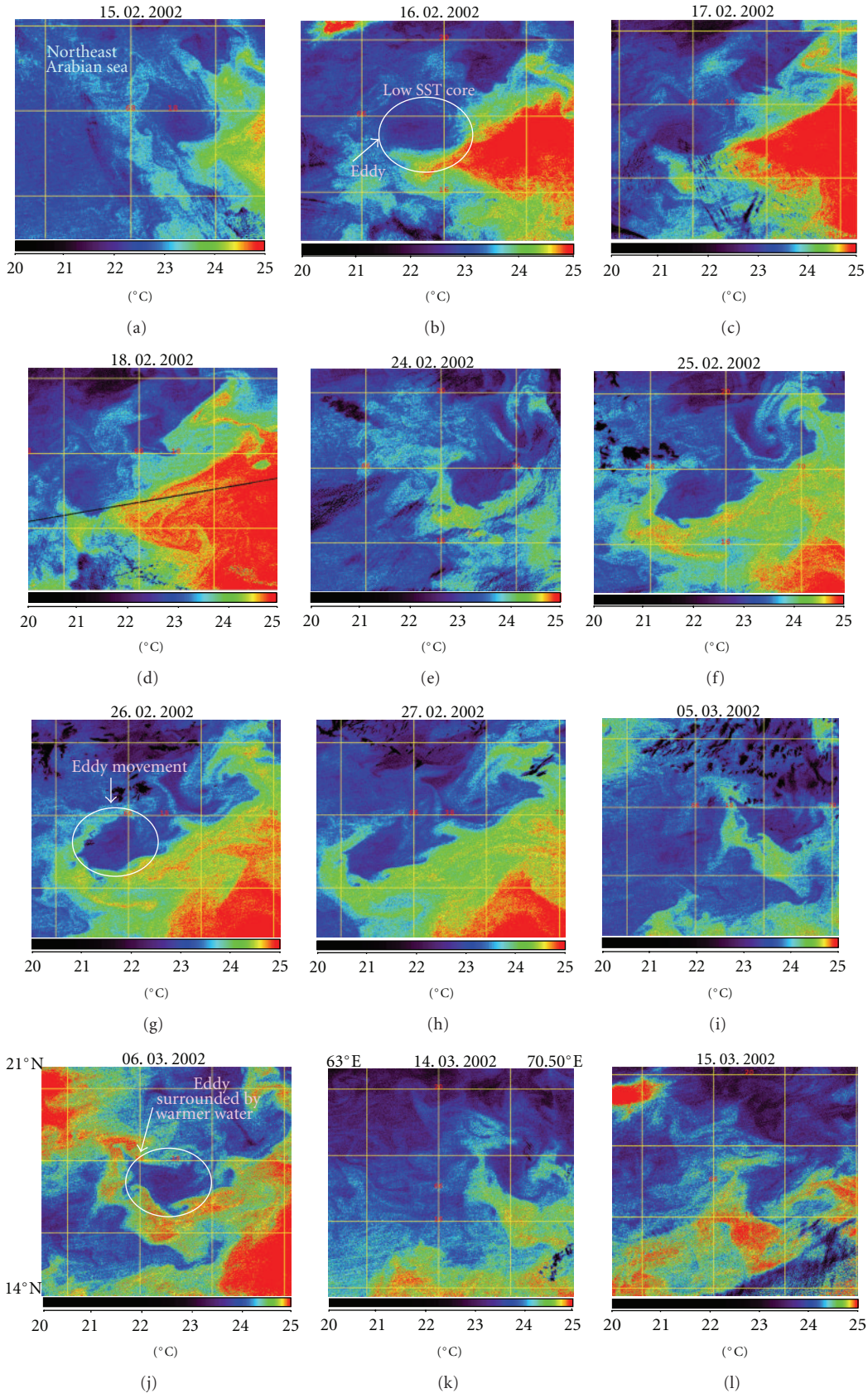

Figure 3: NOAA-AVHRR retrieved Sea Surface Temperature (SST) images showing oceanic eddy and its subsequent stages in the Arabian Sea during February-March 2002.

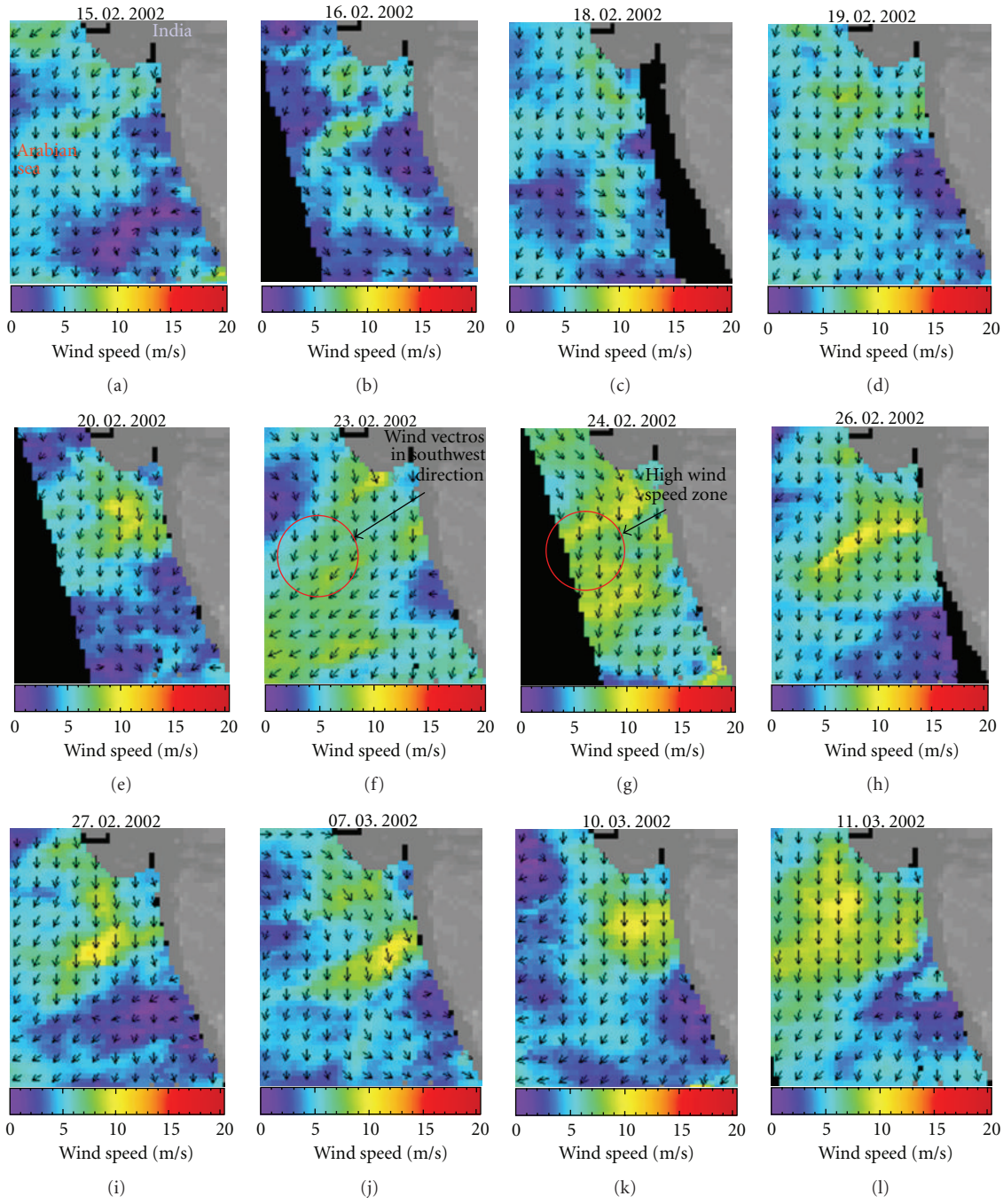

Figure 4: NASA-Quickscat retrieved wind vector data over northern Arabian Sea during February-March 2002.

along the eddy. Wind speed was seen high around 8–10 m/sec in the eddy and surrounding zone, but the wind vector was not seen prominently. As the eddy was of small scale and of lower magnitude, the wind vector of comparatively lower resolution has not made much impact and was not identified in the 360 meter high-resolution OCM–derived eddy region 65–67°E latitude and 17-18°N longitude. Still the high wind speed (8–10 m/sec) has been observed around the above zone in the study area, northeast Arabian Sea. The wind vector showed its movement in southeast to southwest direction, which might have helped in churning the surface water and eddy formation. The increase in the chlorophyll concentration (0.80 to 1.50 mg/m^3) at the core of eddy was evident, where the SST was decreasing (24.5°C to 23°C) and the wind speed was high (8–10 m/sec). These were the prevailing conditions and observations along the eddy. The link between the chlorophyll, SST, and wind speed/vector has been understood and hence the validity of biological

productivity in the northeast Arabian Sea, during this winter cooling period of northeast monsoon.

The northern Arabian Sea is one of the most biologically productive ocean regions [38]. Dynamics and thermodynamics of the surface layer of the Arabian Sea are dominated by the monsoon-related annual cycle of air-sea momentum and heat fluxes [39]. The northern Arabian Sea is renowned for complicated flow pattern consisting of several eddies [40] and the water mass structure in the Arabian Sea is complex [41]. During the northeast monsoon (November–February), the winds blow from the northeast and have maximum wind stress magnitudes about $2\,\text{dyne}\cdot\text{cm}^{-2}$ [39]. The circulation pattern consists of several eddies and meanders, with a pronounced anticyclonic eddy around 24°N and 64°E. In general, eddies appear to have appreciable deep vertical extension [42]. The eddy circulation is attributed to the influence of bottom topography, which is marked by depressions and rises [43]. Upwelling in the eastern Arabian Sea occurs during southwest monsoon during July–September [39]. During the winter, the northeast monsoon during February, the convection process tends to generate eddies and brings up bottom water with nutrient rich water to make the region cooler and productive [44] and even the wind plays a major role to enhance the cooling process and algal blooming [45]. So, the eddy has relation to convection and wind pattern as well, so those eddies can be termed as convective eddies.

The winter convection in the northeastern Arabian sea leads to elevated pigment values, as does even modest mixing during southwest (summer) monsoon. This is due to winter cooling due to high evaporation, mixing, and convection processes leading to the nutrient injection to the surface layer. During winter the northern Arabian Sea (especially north of 10°N) experiences a net heat loss, about $140\,\text{W/m}^2$ [44]. The cool dry continental air brought by the prevailing north-east monsoon winds enhances evaporation, leading to surface cooling [38]. Apart from the cooling due to evaporation, the decrease in insolation (net short wave radiation) from $220\,\text{W/m}^2$ during October to about $160\,\text{W/m}^2$ during January also contributes to the further cooling of the surface waters [46]. Thus, the observed reduction in SST (by about 4°C) [47] and creation of a deep mixed layer depth (MLD), in the northern Arabian Sea during winter is forced by combination of enhanced evaporation and decrease in the insolation. In fact, this starts during December and persists till the end of February [44]. Accordingly, the northern Arabian Sea, north of 15°N, experiences cooling and densification, which leads to sinking and convective mixing and injects nutrients into the surface layers from thermocline region. Off India, the bloom occurs towards the beginning of the February because the mixed layer detrains earlier than the other regions. This occurs when the mixed layer detrains after a period of entrainment, during which the layer is thick enough to inhabit phytoplankton growth. Detrainment occurs when there is a decrease in turbulent mixing (when the wind weakens or there is surface heating). The deeper mixed layer which often being present after winter time cooling. As fluid detrains from the mixed layer, a fossil layer is created that thickens in time. Detrainment blooms tend to be highly productive because detrainment results in a thin mixed layer, which intensifies the depth-averaged light intensity and favors phytoplankton growth. The bloom-forming features of the phytoplankton due to eddy observed in the present study are in good agreement with the previous works carried out by several researchers in the same regions, along the northern Arabian Sea during the winter monsoon period [44, 48]. This type of cold core/anticyclonic eddy is likely to occur regularly during late winter/spring as a result of the prevailing climatic conditions at that time of the year.

Entrainment of water reduces the surface water column temperature [45]. During summer monsoon (July–September), upwelling/Ekman pumping/lateral advection processes are mostly relevant to the eastern Arabian Sea. But, during the winter/northeast monsoon (January–March), it is the convection and entrainment/detrainment processes forced by intraseasonal wind induces the eddy, as evident from the current study. It is observed that in the northeast Arabian Sea the eddy is formed due to convective processes from bottom and water column, during the winter monsoon period in February. The processes like detrainment and entrainment play role in bringing up the cooler water and the bottom nutrient to surface and hence the algal blooming and increase in the chlorophyll concentration. The information on oceanic eddies are very much required in studies like acoustic propagation, optimum ship route planning, fishery forecasting and zoning, delineating good/bad monsoon years, heat transport, and so forth.

8. Conclusion

The present study on the detection and monitoring the phases of eddy in the Arabian Sea water gives an insight into the utilization of multisensor satellites (IRS-P4 OCM, NOAA-AVHRR, NASA-Quickscat) data-retrieved multiparameters like the chlorophyll, SST, and wind vector field respectively. The eddy is well understood as a cold core type from the IRS-P4 OCM multidate chlorophyll images interpretation and is well supported from the NOAA-AVHRR-retrieved SST images information. The rotational movement of the eddy was appearing in clockwise direction in chlorophyll images, which was confirmed with the information obtained from the Quickscat-retrieved wind vectors, as clockwise moving anticyclonic eddy. The increase in the chlorophyll concentration at the core of eddy was evident, where the SST was decreasing and the wind speed was high. The link between the three parameters (chlorophyll, SST and wind) has been understood and the enhancement in the biological productivity has been resulted with effect of the cold core eddy and its churning phases. The eddy observed to be regulated by the processes like convection and hence the entrainment and detrainment to enhance the surface water chlorophyll with the bottom water nutrients. So, the detailed knowledge about the eddies, their types, circulation patterns, and finally their role in regulating the marine living resources up to the secondary production in terms of the increase in fish catch details in the Arabian Sea water, in different regions and seasons are essential.

Acknowledgments

The authors are thankful to the Director of, Space Applications Centre for providing necessary guidance and facilities for carrying out the work. The Quickscat wind vector data provided by PO.DAAC, JPL/NASA are sincerely acknowledged.

References

[1] Yi and Chao, http://www.jpl.nasa.gov/releases/2002/release_2002_175.html.

[2] D. Tang, H. Kawamura, and A. J. Luis, "Short-term variability of phytoplankton blooms associated with a cold eddy in the northwestern Arabian Sea," *Remote Sensing of Environment*, vol. 81, no. 1, pp. 82–89, 2002.

[3] C. S. Yentsch, "The influence of phytoplankton pigments on the colour of sea water," *Deep Sea Research*, vol. 7, no. 1, pp. 1–9, 1960.

[4] C. J. Lorenzen, "Extinction of light in the ocean by phytoplankton," *Journal du Conseil International pour l'Exploration de la Mer*, vol. 34, pp. 262–267, 1972.

[5] R. C. Smith, J. Marra, M. J. Perry et al., "Estimation of a photon budget for the upper ocean in the Sargasso Sea," *Limnology & Oceanography*, vol. 34, no. 8, pp. 1673–1693, 1989.

[6] J. Aiken, G. F. Moore, and P. M. Holligan, "Remote sensing of oceanic biology in relation to global climate change," *Journal of Phycology*, vol. 28, no. 5, pp. 579–590, 1992.

[7] B. G. Mitchell, "Coastal Zone Color Scanner retrospective," *Journal of Geophysical Research*, vol. 99, no. 4, pp. 7291–7292, 1994.

[8] J. A. Yoder, "Chapter 12 An overview of temporal and spatial patterns in satellite-derived chlorophyll-a imagery and their relation to ocean processes," *Elsevier Oceanography Series*, vol. 63, pp. 225–238, 2000.

[9] R. K. Sarangi, P. Chauhan, and S. R. Nayak, "Phytoplankton bloom monitoring in the offshore water of northern Arabian Sea using IRS-P4 OCM satellite data," *Indian Journal of Marine Sciences*, vol. 30, no. 4, pp. 214–221, 2001.

[10] J. Hu, J. Gan, Z. Sun, J. Zhu, and M. Dai, "Observed three-dimensional structure of a cold eddy in the southwestern South China Sea," *Journal of Geophysical Research*, vol. 116, Article ID C05016, pp. 1–11, 2011.

[11] C. Chavanne, P. Flament, R. Lumpkin, B. Dousset, and A. Bentamy, "Scatterometer observations of wind variations by oceanic islands: implications for wind driven ocean circulation," *Journal of Remote Sensing*, vol. 28, pp. 466–474, 2002.

[12] C. Dong, T. Mavor, F. Nencioli et al., "An oceanic cyclonic eddy on the lee side of Lanai Island, Hawaii," *Journal of Geophysical Research C*, vol. 114, no. 10, Article ID C10008, 13 pages, 2009.

[13] T. D. Dickey, F. Nencioli, V. S. Kuwahara et al., "Physical and bio-optical observations of oceanic cyclones west of the island of Hawai'i," *Deep-Sea Research Part II*, vol. 55, no. 10–13, pp. 1195–1217, 2008.

[14] V. S. Kuwahara, F. Nencioli, T. D. Dickey, Y. M. Rii, and R. R. Bidigare, "Physical dynamics and biological implications of Cyclone Noah in the lee of Hawai'i during E-Flux I," *Deep-Sea Research Part II*, vol. 55, no. 10–13, pp. 1231–1251, 2008.

[15] S. L. Brown, M. R. Landry, K. E. Selph, E. Jin Yang, Y. M. Rii, and R. R. Bidigare, "Diatoms in the desert: Plankton community response to a mesoscale eddy in the subtropical North Pacific," *Deep-Sea Research Part II*, vol. 55, no. 10–13, pp. 1321–1333, 2008.

[16] M. R. Landry, M. Decima, M. P. Simmons, C. C. S. Hannides, and E. Daniels, "Mesozooplankton biomass and grazing responses to Cyclone *Opal*, a subtropical mesoscale eddy," *Deep-Sea Research Part II*, vol. 55, no. 10–13, pp. 1378–1388, 2008.

[17] C. R. Benitez-Nelson, R. R. Bidigare, T. D. Dickey et al., "Mesoscale eddies drive increased silica export in the subtropical Pacific ocean," *Science*, vol. 316, no. 5827, pp. 1017–1021, 2007.

[18] R. R. Bidigare, C. Benitez-Nelson, C. L. Leonard et al., "Influence of a cyclonic eddy on microheterotroph biomass and carbon export in the lee of Hawaii," *Geophysical Research Letters*, vol. 30, no. 6, article 1318, 4 pages, 2003.

[19] R. D. Vaillancourt, J. Marra, M. P. Seki, M. L. Parsons, and R. R. Bidigare, "Impact of a cyclonic eddy on phytoplankton community structure and photosynthetic competency in the subtropical North Pacific Ocean," *Deep-Sea Research Part I: Oceanographic Research Papers*, vol. 50, no. 7, pp. 829–847, 2003.

[20] M. P. Seki, J. J. Polovina, R. E. Brainard, R. R. Bidigare, C. L. Leonard, and D. G. Foley, "Biological enhancement at cyclonic eddies tracked with GOES thermal imagery in Hawaiian waters," *Geophysical Research Letters*, vol. 28, no. 8, pp. 1583–1586, 2001.

[21] T. D. Dickey and R. R. Bidigare, "Interdisciplinary oceanographic observations: the wave of the future," *Scientia Marina*, vol. 69, supplement 1, pp. 23–42, 2005.

[22] J. A. Yoder, C. R. McClain, G. C. Feldman, and W. E. Esaias, "Annual cycles of phytoplankton chlorophyll concentrations in the global ocean: a satellite view," *Global Biogeochemical Cycles*, vol. 7, no. 1, pp. 181–193, 1993.

[23] H. Kawamura and OCTS Team, "OCTS mission overview," *Journal of Oceanography*, vol. 54, no. 5, pp. 383–399, 1998.

[24] D. L. Tang, I. H. Ni, D. R. Kester, and F. E. Müller-Karger, "Remote sensing observations of winter phytoplankton blooms southwest of the Luzon Strait in the South China Sea," *Marine Ecology Progress Series*, vol. 191, pp. 43–51, 1999.

[25] K. Banse and D. C. English, "Geographical differences in seasonality of CZCS-derived phytoplankton pigment in the Arabian Sea for 1978–1986," *Deep-Sea Research Part II*, vol. 47, no. 7-8, pp. 1623–1677, 2000.

[26] G. Zibordi, F. Parmiggiani, and L. Alberotanza, "Application of aircraft multispectral scanner data to algae mapping over the venice lagoon," *Remote Sensing of Environment*, vol. 34, no. 1, pp. 49–54, 1990.

[27] P. Lavery, C. Pattiaratchi, A. Wyllie, and P. Hick, "Water quality monitoring in estuarine waters using the Landsat thematic mapper," *Remote Sensing of Environment*, vol. 46, no. 3, pp. 268–280, 1993.

[28] R. R. Navalgund and A. S. Kiran Kumar, "IRS-P4 Ocean Color Monitor (OCM)," Technical Note, 1999.

[29] H. W. Gordon and M. Wang, "Retrieval of water-leaving radiance and aerosol optical thickness over the oceans with SeaWiFS: a preliminary algorithm," *Applied Optics*, vol. 33, no. 3, pp. 443–452, 1994.

[30] M. Mohan, P. Chauhan, M. Raman et al., "Initial results of MOS validation experiment over the Arabian sea, atmospheric correction aspects," in *Proceedings of the 1st International Workshop on MOS-IRS and Ocean Color*, pp. 1–11, DLR, Berlin, Germany, 1997.

[31] P. Chauhan, C. R. C. Nagur, M. Mohan, S. R. Nayak, and R. R. Navalgund, "Surface chlorophyll-a distribution in Arabian Sea and Bay of Bengal using IRS-P4 Ocean Color Monitor (OCM) satellite data," *Current Science*, vol. 80, pp. 40–41, 2001.

[32] J. E. O'Reilly, S. Maritorena, B. G. Mitchell et al., "Ocean color chlorophyll algorithms for SeaWiFS," *Journal of Geophysical Research C*, vol. 103, no. 11, pp. 24937–24953, 1998.

[33] P. Chauhan, M. Mohan, R. K. Sarngi, B. Kumari, S. Nayak, and S. G. P. Matondkar, "Surface chlorophyll a estimation in the Arabian Sea using IRS-P4 Ocean Colour Monitor (OCM) satellite data," *International Journal of Remote Sensing*, vol. 23, no. 8, pp. 1663–1676, 2002.

[34] E. P. McClain, "Overview of satellite data applications in the climate and earth sciences laboratory of NOAA's National Environment al Satellite, data and information services," in *Proceedings of the US-Indo Symposium-cum-Workshop on Remote Sensing Fundamentals and Applications*, p. 247, Ahmedabad, India, 1985.

[35] E. P. McClain, W. G. Pichel, and C. C. Walton, "Comparative performance of AVHRR-based multichannel sea surface temperatures," *Journal of Geophysical Research*, vol. 90, no. 6, pp. 11587–11601, 1985.

[36] C. C. Walton, "Nonlinear multichannel algorithms for estimating sea surface temperature with AVHRR satellite data," *Journal of Applied Meteorology*, vol. 27, pp. 115–124, 1988.

[37] M. V. Rao, A. Narendra Nath, T. D. Suhasini, D. Jogendra Nath, and K. H. Rao, "A comparison of satellite MCSST with ship measured SST in the North Indian Ocean," *Geocarto International*, vol. 12, no. 2, pp. 13–22, 1997.

[38] M. Madhupratap, S. P. Kumar, P. M. A. Bhattathiri et al., "Mechanism of the biological response to winter cooling in the northeastern Arabian Sea," *Nature*, vol. 384, no. 6609, pp. 549–552, 1996.

[39] S. R. Shetye, A. D. Gouveia, and S. S. C. Shenoi, "Circulation and water masses of the Arabian Sea," in *Biogeochemistry of the Arabian Sea*, D. Lal, Ed., pp. 9–25, Indian Academy of Sciences, Phototypeset at Thomson Press, New Delhi, India, 1994.

[40] E. Böhm, J. M. Morrison, V. Manghnani, H. S. Kim, and C. N. Flagg, "The Ras al Hadd Jet: remotely sensed and acoustic Doppler current profiler observations in 1994-1995," *Deep-Sea Research Part II*, vol. 46, no. 8-9, pp. 1531–1549, 1999.

[41] J. M. Morrison, L. A. Codispoti, S. Gaurin, B. Jones, V. Manghnani, and Z. Zheng, "Seasonal variation of hydrographic and nutrient fields during the US JGOFS Arabian Sea Process Study," *Deep-Sea Research Part II*, vol. 45, no. 10-11, pp. 2053–2101, 1998.

[42] S. Z. Qasim, "Oceanography of the northern Arabian Sea," *Deep Sea Research Part A*, vol. 29, no. 9, pp. 1041–1068, 1982.

[43] V. K. Das, A. D. Gouveia, and K. K. Varma, "Circulation and water characteristics on isanosteric surfaces in the northern Arabian Sea," *Indian Journal of Marine Sciences*, vol. 9, pp. 156–165, 1980.

[44] S. Prasanna Kumar and T. G. Prasad, "Winter cooling in the northern Arabian Sea," *Current Science*, vol. 71, no. 11, pp. 834–841, 1996.

[45] K. Banse and D. C. English, "Geographical differences in seasonality of CZCS-derived phytoplankton pigment in the Arabian Sea for 1978–1986," *Deep-Sea Research Part II*, vol. 47, no. 7-8, pp. 1623–1677, 2000.

[46] S. Hasternath and P. J. Lamb, *Climatic Atlas of the Indian Ocean. Part I: Surface Climate and Atmospheric Circulation*, University of Wisconsin Press, Madison, Wis, USA, 1979.

[47] S. Hasternath and L. L. Greischar, *Climatic Atlas of the Indian Ocean, Part III: Upper–Ocean Structure*, The University of Wisconsin Press, Madison, Wis, USA, 1989.

[48] K. Banse and C. R. McClain, "Winter blooms of phytoplankton as observed by the Coastal Zone Color Scanner," *Marine Ecology Progress Series*, vol. 34, pp. 201–211, 1986.